Computer Assisted Mechanics and Engineering Sciences, **13**: 565–574, 2006.

Numerical modelling of coupled heat, moisture and salt transport in porous materials

Marcin Koniorczyk, Dariusz Gawin
Chair of Building Physics and Building Materials, Technical University of Łódź
Al. Politechniki 6, 90-924 Łódź, Poland

(Received in the final form October 18, 2006)

A mathematical model describing coupled heat, moisture and salt transport in porous materials is presented. Salt dissolved in water can be transported due to various mechanisms: dispersion caused by the salt concentration gradient, and advection resulting from the capillary pressure gradient. The influence of salt on the physical properties of water such as density and dynamic viscosity is also considered. The isotherms of water sorption are modified to take into account both osmosis and effects of the salt presence on the surface tension and contact angle. Salt precipitation in the state of thermodynamic equilibrium between dissolved and crystallized salt is also considered. Finally, the model equations were discretized in space by means of FEM and the HMTRA-SALT software was developed. An example concerning a wall drying process was numerically solved to show the robustness of the code.

Keywords: porous materials, salt transport, hydrodynamic dispersion, coupled transport

1. Introduction

The study of mass and energy transport in porous media is very important in many industrial and environmental disciplines. Abundance of applications can be found in the fields of building physics (thermal and hygric performance of buildings), petroleum production (oil flow in reservoirs), geotechnics (migration of hazardous wastes in soil or saltwater flow), concrete (prediction of a service life for concrete structures, corrosion of steel bars initiated by compounds dissolved in porous liquid), conservation of historical monuments (efflorescence on historic surfaces: frescos and paintings, deterioration of sandstone, etc.).

In this paper the modelling of salt transport in non-isothermal, partially or fully saturated, porous materials is described. It is assumed that only one salt may be dissolved in water which fills pores. Salt strongly affects the liquid moisture behaviour. Water properties (density, dynamic viscosity) depend on the salt concentration. Salt influences hygroscopic sorption and water retention characteristics by changing the surface tension and contact angle. The hysteresis in the moisture retention function is excluded here. Salt precipitation and its influence on moisture transport are considered. Precipitation of a salt may cause crystallisation pressure in interface layer and block pores, which prevents moisture from moving. During the crystallisation process additional heat is released. The formulation presented in this paper is applicable in building physics, and after same minor modifications, in other scientific fields as well.

The derivation of mathematical model describing coupled energy, moisture and salt transport in deformable porous material and the numerical solution of the governing equations are presented in this paper. The model, formulated by Gawin and Schrefler [3], Gawin [4], and Lewis and Schrefler [9], has been extended with the salt mass balance equation. The other equations have been modified appropriately. This paper focuses on the salt influence upon the transport phenomena in porous materials. The averaging theory by Hassanizadeh and Gray [5–7] is applied to formulate macroscopic

balance equations. This is the scale where all physical properties of the medium are experimentally measured to obtain the constitutive relations.

2. Mathematical model

Porous material is modelled as a multi-phase medium, which is assumed to be locally in a thermodynamic equilibrium state. The voids of skeleton are filled partly with a liquid phase consisting of water and dissolved salt, partly with a gaseous phase consisting of dry air and vapour and partly with precipitated salt. The liquid phase consists of bound water, which is present in the whole range of water content, and capillary water, which appears when water content exceeds the upper limit of hygroscopic region – S_{ssp}. The liquid content is described by the degree of saturation – S_{w}. Salt appears in two phases: one is the salt dissolved in the liquid phase, described by the mass concentration – ω, the other is precipitated salt, described by the degree of pore saturation with the precipitated salt – S_{p}. The gas is assumed to be an ideal gas. The chosen primary variables of the model are: gas pressure p^{g}, capillary pressure $p^{\mathrm{c}} = p^{\mathrm{g}} - p^{\mathrm{w}}$, where p^{w} denotes water pressure, temperature T, salt mass concentration in the solution ω, displacement vector of the solid matrix $\mathbf{u}$, for two-dimensional problem $\mathbf{u} = [u_x, u_y]$. The model consists of five balance equations: water mass balance, dry air mass balance, salt mass balance, energy balance and linear momentum balance.

Using the Volume Averaging Theorem also called hybrid mixture theory formulated by Gray and Hassanizadeh [5–7] five macroscopic balance equations will be derived. At the macroscopic scale one can measure all necessary coefficients and materials properties (density of materials, water dynamic viscosity, permeability, diffusivity factors, characteristic lengths of dispersion) experimentally. There will be presented only the final form of the balance equations and all appearing coefficients will be discussed in the article.

The mass balance equation of dry air includes both diffusive (the third term in the l.h.s.) and advective (the last term in the l.h.s.) components of the mass fluxes, influence of precipitated salt is also considered,

$$n\frac{\partial}{\partial t}(S_{\mathrm{g}}\rho^{\mathrm{a}}) - \beta_{\mathrm{s}}S_{\mathrm{g}}\rho^{\mathrm{a}}(1-n)\frac{\partial T}{\partial t} + \operatorname{div}(\mathbf{J}_{\mathrm{g}}^{\mathrm{a}}) + S_{\mathrm{g}}\rho^{\mathrm{a}}\operatorname{div}\left(\frac{\partial \mathbf{u}}{\partial t}\right) + \operatorname{div}(nS_{\mathrm{g}}\rho^{\mathrm{a}}\mathbf{v}^{\mathrm{gs}}) = 0, \tag{1}$$

where t – time, β_{s} – cubic thermal expansion coefficient of the solid skeleton, $\mathbf{v}^{\mathrm{gs}}$ – gas velocity relative to the solid skeleton, $\mathbf{J}_{\mathrm{g}}^{\mathrm{a}}$ – diffusive flux of dry air, ρ – density of the phase marked by the appropriate subscript: w – liquid phase, a - dry air, v – vapour, s – solid skeleton, p – precipitated salt, g – gas phase; S_{g} – pores saturation with the gaseous phase characterized by $S_{\mathrm{g}} = 1 - S_{\mathrm{w}} - S_{\mathrm{p}}$.

The mass balance of liquid water and vapour, summed together to eliminate the source term related to evaporation-concentration or adsorption-desorption, form the mass balance equation of water species,

$$\begin{aligned} &n\frac{\partial}{\partial t}(S_{\mathrm{w}}\rho^{\mathrm{w}}) + n\frac{\partial}{\partial t}(S_{\mathrm{g}}\rho^{\mathrm{v}}) - \beta_{\mathrm{s}}(1-n)\left(S_{\mathrm{g}}\rho^{\mathrm{v}} + S_{\mathrm{w}}\rho^{\mathrm{w}}\right)\frac{\partial T}{\partial t} \\ &\quad + \left(S_{\mathrm{w}}\rho^{\mathrm{w}} + S_{\mathrm{g}}\rho^{\mathrm{v}}\right)\operatorname{div}\left(\frac{\partial \mathbf{u}}{\partial t}\right) + \operatorname{div}(nS_{\mathrm{w}}\rho^{\mathrm{w}}\mathbf{v}^{\mathrm{ws}}) + \operatorname{div}(nS_{\mathrm{g}}\rho^{\mathrm{v}}\mathbf{v}^{\mathrm{gs}}) + \operatorname{div}(\mathbf{J}_{\mathrm{g}}^{\mathrm{v}}) = 0, \end{aligned} \tag{2}$$

where $\mathbf{v}^{\mathrm{ws}}$ – fluid phase velocity relative to the solid skeleton, $\mathbf{J}_{\mathrm{g}}^{\mathrm{v}}$ – diffusive flux of water vapour.

It is assumed in the formulation, that salt influences the water density, dynamic viscosity and water retention characteristic. The sources or sinks of dissolved salt due to the precipitation process are also considered (the third term in the l.h.s.). The mass balance of the salt dissolved in the fluid phase is expressed as

$$\begin{aligned} &n\frac{\partial}{\partial t}(\rho^{\mathrm{w}}\omega S_{\mathrm{w}}) - S_{\mathrm{w}}\omega\rho^{\mathrm{w}}\beta_{\mathrm{s}}(1-n)\frac{\partial T}{\partial t} + n\rho^{\mathrm{p}}\frac{\partial S_{\mathrm{p}}}{\partial t} \\ &\quad + S_{\mathrm{w}}\omega\rho^{\mathrm{w}}\operatorname{div}\left(\frac{\partial \mathbf{u}}{\partial t}\right) + \operatorname{div}(nS_{\mathrm{w}}\omega\rho^{\mathrm{w}}\mathbf{v}^{\mathrm{ws}}) + \operatorname{div}(\mathbf{J}) = 0, \end{aligned} \tag{3}$$

where $\mathbf{J}$ – dispersive flux described in the next section.

The enthalpy conservation equation of the multiphase medium, obtained by summing the appropriate balance equations of the constituents includes the heat effects due to phase change of water and heat released during the salt precipitation process (the terms in the r.h.s.), as well as the convectional and latent heat transfer,

$$(\rho C_{\mathrm{p}})_{\mathrm{ef}} \frac{\partial T}{\partial t} + \left(\rho^{\mathrm{w}} C_{\mathrm{p}}^{\mathrm{w}} \mathbf{v}^{\mathrm{ws}} + \rho^{\mathrm{g}} C_{\mathrm{p}}^{\mathrm{g}} \mathbf{v}^{\mathrm{gs}}\right) \cdot \operatorname{grad} T - \operatorname{div}\left(\lambda_{\mathrm{ef}} \operatorname{grad} T\right) = -\dot{m}_{\mathrm{vap}} \Delta H_{\mathrm{vap}} - \dot{m}_{\mathrm{prec}} \Delta H_{\mathrm{prec}}\,, \tag{4}$$

where $(\rho C_{\mathrm{p}})_{\mathrm{ef}}$ – effective thermal capacity of the multiphase domain, C_{p} – isobaric specific heat, λ_{ef} – effective thermal conductivity, ΔH_{vap} – specific enthalpy of phase change of the water, ΔH_{prec} – specific enthalpy of crystallization process, $\dot{m}_{\mathrm{vap}}$ – mass source or sink of vapour related to the evaporation or condensation process, $\dot{m}_{\mathrm{prec}}$ – sink of dissolved salt due to precipitation process.

Introducing Bishop's stress tensor $\boldsymbol{\sigma}''$ [9], called also effective stress tensor responsible for the main deformation (in soil rearrangement of soil particles), the linear momentum conservation equation of the whole medium is given by [4, 9],

$$\operatorname{div}\left(\boldsymbol{\sigma}'' - \alpha \mathbf{I} p^{\mathrm{s}}\right) + \mathbf{g}\left[(1-n)\rho^{\mathrm{s}} + nS_{\mathrm{w}}\rho^{\mathrm{w}} + nS_{\mathrm{g}}\rho^{\mathrm{g}} + nS_{\mathrm{p}}\rho^{\mathrm{p}}\right] = 0, \tag{5}$$

where $\mathbf{I}$ – unit second order tensor, α – Biot's coefficient, $\mathbf{g}$ – acceleration of gravity. Pressure in the solid phase p^s is given by the following formula [9],

$$p^{\mathrm{s}} = p^{\mathrm{g}} - x_{\mathrm{s}}^{\mathrm{ws}} p^{c}, \tag{6}$$

where $x_{\mathrm{s}}^{\mathrm{ws}}$ means the solid surface fraction in contact with the wetting film, depending on the water saturation degree S_{w} of the pores.

3. Constitutive relations

There are many coefficients and expressions describing materials' properties in Eqs. (1)–(5), which must be defined in order to solve the equations. One can obtain them from constitutive and state equations as well as from thermodynamic relationships. These properties should be determined at the macroscopic level from experiments.

The constitutive relationship for the solid skeleton is assumed in the following incremental form [10]

$$\mathrm{d}\boldsymbol{\sigma}'' = \mathbf{D}\left(\mathrm{d}\boldsymbol{\varepsilon} - \mathrm{d}\boldsymbol{\varepsilon}_T - \mathrm{d}\boldsymbol{\varepsilon}_0\right) \tag{7}$$

where $\mathbf{D}$ is the tangent matrix, $\boldsymbol{\varepsilon} = \mathbf{B}\mathbf{u}$ is the relation between the strain tensor $\boldsymbol{\varepsilon}$ and the displacement vector $\mathbf{u}$, $\mathrm{d}\boldsymbol{\varepsilon}_T = \mathbf{I}\beta_{\mathrm{s}}/3\,\mathrm{d}T$ is the strain caused by thermo-elastic expansion, $\mathrm{d}\boldsymbol{\varepsilon}_0$ is the autogeneous strain increment.

The expression describing dispersive flux in Eq. (3) is needed. This flux results from both mechanical dispersion and molecular diffusion [1, 2]. Mechanical dispersion expresses the effect of the microscopic variation of velocity (direction and value) in the vicinity of the considered point. Molecular diffusion is caused by the random motion of molecules in the fluid from regions of higher tracer concentration to regions with a lower one. The hydrodynamic dispersion is modelled using extended linear Fick's law expressed as [1, 2]

$$\mathbf{J} = -\rho^{\mathrm{w}} \mathbf{D}^{d} \cdot \operatorname{grad}(\omega) \tag{8}$$

where $\mathbf{D}^{\mathrm{d}}$ – tensor of hydrodynamic dispersion which may be in indicial notation described as

$$D_{ij}^{\mathrm{d}} = \left(\alpha_T |\mathbf{j}| + nS_{\mathrm{w}} D^{\mathrm{mol}}\right)\delta_{ij} + (\alpha_L - \alpha_T)\frac{j_i j_j}{|\mathbf{j}|} \tag{9}$$

where D^{mol} – coefficient of molecular diffusion, $\mathbf{j}$ – advective flux of liquid phase, α_L – longitudinal dispersivity, α_T – transverse dispersivity, $\delta_{ij} = 1$ when $i = j$ and $\delta_{ij} = 0$ when $i \neq j$. Longitudinal and transversal dispersivity may be determined in an experiment or by solving an appropriate inverse problem.

As a constitutive equation for the capillary water flow and advectional gas flow, the modified Darcy's law is applied,

$$\mathbf{j}^{\mathrm{ws}} = \frac{\mathbf{k}k^{\mathrm{rw}}}{\mu^{\mathrm{w}}} \left[\mathrm{grad}\,(p^{\mathrm{c}}) - \mathrm{grad}\,(p^{\mathrm{g}}) + \rho^{\mathrm{w}}\mathbf{g}\right], \tag{10}$$

$$\mathbf{j}^{\mathrm{gs}} = \frac{\mathbf{k}k^{\mathrm{rg}}}{\mu^{\mathrm{g}}} \left[\mathrm{grad}\,(p^{\mathrm{g}}) + \rho^{\mathrm{g}}\mathbf{g}\right], \tag{11}$$

where $\mathbf{k}$ – intrinsic permeability tensor, μ^{w} – dynamic viscosity of the liquid phase, μ^{g} – dynamic viscosity of the gaseous phase, k^{rw} – relative permeability of the liquid phase, k^{rg} – relative permeability of the gaseous phase. The concept of relative permeability extends the validity of Darcy's law to the partially saturated state. Relative permeability may be defined with a sufficient accuracy as a function of the degree of saturation of pores with an appropriate phase.

For the physically adsorbed water diffusion, the Fick's law is applied [8],

$$\mathbf{j}^{\mathrm{wd}} = -\mathbf{D}_{\mathrm{b}}\,\mathrm{grad}\,(S_{\mathrm{w}}), \tag{12}$$

where $\mathbf{D}_{\mathrm{b}}$ – bound water diffusion tensor.

The diffusion process in the binary gas mixture consisting of the dry air and water vapour is described by the Fick's law [4],

$$\mathbf{J}^{\mathrm{a}}_{\mathrm{g}} = -\mathbf{J}^{\mathrm{v}}_{\mathrm{g}} = \rho^{\mathrm{g}} \frac{M_{\mathrm{a}} M_{\mathrm{w}}}{M_{\mathrm{g}}^2} \mathbf{D}^{\mathrm{g}}_{\mathrm{v}}\,\mathrm{grad}\left(\frac{p^{\mathrm{v}}}{p^{\mathrm{g}}}\right), \tag{13}$$

where $\mathbf{D}^{\mathrm{g}}_{\mathrm{v}}$ – effective diffusivity tensor of vapour in the air, M_{a} – molar mass of dry air, M_{w} – molar mass of water, M_{g} – molar mass of the gas phase.

Salt dissolved in the liquid phase influences its density and dynamic viscosity, which appear in the macroscopic balance equations as well as in some constitutive equations. It is assumed that liquid density depends on temperature, pressure and salt concentration, according to the expression [8]

$$\rho^{\mathrm{w}} = \rho^{\mathrm{w}}_0 \exp\left[1 - \beta_{\mathrm{w}}(T - T_0) + \beta_{\mathrm{p}}(p^{\mathrm{w}} - p^{\mathrm{atm}}) + \gamma\omega\right] \tag{14}$$

where ρ^{w}_0 – density of the pure water at atmospheric pressure and temperature $T = 273.15$ K, β_{w}, β_{p} – material coefficients, $\gamma = 0.69$ [8]. The liquid dynamic viscosity is described by [10]

$$\mu = \mu_0(1 + 1.85\omega - 4.1\omega^2 + 44.5\omega^3) \tag{15}$$

where μ_0 – dynamic viscosity of pure water, depending on temperature.

3.1. Boundary and initial condition

To solve the model differential equations (4)–(8) together with constitutive relations presented in this section one must formulate initial and boundary conditions.

The initial conditions specify entire fields of gas pressure, capillary pressure, salt concentration, temperature and displacements over the analysed domain Ω together with its boundary Γ ($\Gamma = \Gamma_\pi \cup \Gamma^q_\pi$, $\pi = \mathrm{g}, \mathrm{c}, \omega, T, \mathbf{u}$) at the beginning of the process, $t = 0$,

$$p^{\mathrm{g}} = p^{\mathrm{g}}_0\,, \quad p^{\mathrm{c}} = p^{\mathrm{c}}_0\,, \quad \omega = \omega_0\,, \quad T = T_0\,, \quad \mathbf{u} = \mathbf{u}_0\,, \qquad \mathbf{x} \in \Omega, \quad t = 0. \tag{16}$$

The boundary conditions can be of Dirichlet's type on Γ_π,

$$\begin{aligned} p^{\mathrm{g}}(t) &= \hat{p}^{\mathrm{g}} \quad \text{on } \Gamma_{\mathrm{g}}; \\ p^{\mathrm{c}}(t) &= \hat{p}^{\mathrm{c}} \quad \text{on } \Gamma_{\mathrm{c}}; \\ \omega(t) &= \hat{\omega} \quad \text{on } \Gamma_\omega; \\ T(t) &= \hat{T} \quad \text{on } \Gamma_T; \\ \mathbf{u}(t) &= \hat{\mathbf{u}} \quad \text{on } \Gamma_u, \end{aligned} \tag{17}$$

or of Neumann's type on Γ_π^q,

$$\begin{aligned} &(nS_{\mathrm{g}}\rho^{\mathrm{a}}\mathbf{v}^{\mathrm{gs}} + \mathbf{J}_{\mathrm{g}}^{\mathrm{a}}) \cdot \mathbf{n} = q^{\mathrm{a}} && \text{on } \Gamma_{\mathrm{g}}^q; \\ &(nS_{\mathrm{w}}\rho^{\mathrm{w}}\omega\mathbf{v}^{\mathrm{ws}} + \mathbf{J}) \cdot \mathbf{n} = q^{\omega} && \text{on } \Gamma_\omega^q; \\ &\left(nS_{\mathrm{w}}\rho^{\mathrm{w}}\mathbf{v}^{\mathrm{ws}} + nS_{\mathrm{g}}\rho^{\mathrm{v}}\mathbf{v}^{\mathrm{gs}} + \mathbf{J}_{\mathrm{g}}^{\mathrm{v}}\right) \cdot \mathbf{n} = q^{\mathrm{v}} + q^{\mathrm{w}} + \beta_c(\rho^{\mathrm{v}} - \rho_\infty^\nu) && \text{on } \Gamma_c^q; \\ &(nS_{\mathrm{w}}\rho^{\mathrm{w}}\mathbf{v}^{\mathrm{ws}}\Delta H_{\mathrm{vap}} - \lambda_{\mathrm{ef}} \operatorname{grad} T) \cdot \mathbf{n} = q^T + \alpha_c(T - T_\infty) && \text{on } \Gamma_T^q; \\ &\boldsymbol{\sigma} \cdot \mathbf{n} = \hat{\mathbf{t}} && \text{on } \Gamma_u^q, \end{aligned} \tag{18}$$

where $\mathbf{n}$ – unit vector normal to the boundary surface, q^{a}, q^{w}, q^{v}, q^{ω}, q^T – fluxes of dry air, water, vapour, salt and heat, $\hat{\mathbf{t}}$ – imposed traction, α_{c} – convective heat transfer coefficient, β_{c} – convective mass transfer coefficient, ρ_∞^ν – mass concentration of water vapour in the far field of undisturbed gas phase, T_∞ – temperature in the far field of undisturbed gas phase.

4. Numerical solution

In order to solve the formulated equations a computer program has been developed. Discretization of the model equations in space is carried out using the Finite Element Method [14]. The unknown variables are expressed by their nodal values and appropriate shape functions,

$$\begin{aligned} p^{\mathrm{g}}(\mathbf{x},t) &= \mathbf{N}_{\mathrm{g}}(\mathbf{x})\,\bar{\mathbf{p}}^{\mathrm{g}}(t), \\ T(\mathbf{x},t) &= \mathbf{N}_T(\mathbf{x})\,\bar{\mathbf{T}}(t), \\ p^c(\mathbf{x},t) &= \mathbf{N}_c(\mathbf{x})\,\bar{\mathbf{p}}^c(t), \\ \mathbf{u}(\mathbf{x},t) &= \mathbf{N}_u(\mathbf{x})\,\bar{\mathbf{u}}(t), \\ \omega(\mathbf{x},t) &= \mathbf{N}_\omega(\mathbf{x})\,\bar{\omega}(t). \end{aligned} \tag{19}$$

In the formulation $C^{(1)}$ continuity of the interpolating functions is required.

The variational or weak form of the heat and mass transfer equations, applying also state and conservation relations required to complete the model, was obtained by means of Galerkin's method (weighted residual method), and can be expressed in a matrix form as

$$\mathbf{C}\frac{\partial \mathbf{x}}{\partial t} + \mathbf{K}\,\mathbf{x} = \mathbf{f} \tag{20}$$

where

$$\mathbf{C} = \begin{bmatrix} \mathbf{C}_{\mathrm{gg}} & \mathbf{C}_{\mathrm{gc}} & \mathbf{C}_{\mathrm{g}\omega} & \mathbf{C}_{\mathrm{g}t} & \mathbf{C}_{\mathrm{g}u} \\ \mathbf{0} & \mathbf{C}_{\mathrm{cc}} & \mathbf{C}_{\mathrm{c}\omega} & \mathbf{C}_{\mathrm{c}t} & \mathbf{C}_{\mathrm{c}u} \\ \mathbf{0} & \mathbf{C}_{\omega\mathrm{c}} & \mathbf{C}_{\omega\omega} & \mathbf{C}_{\omega t} & \mathbf{C}_{\omega u} \\ \mathbf{0} & \mathbf{C}_{t\mathrm{c}} & \mathbf{C}_{t\omega} & \mathbf{C}_{tt} & \mathbf{C}_{tu} \\ \mathbf{0} & \mathbf{0} & \mathbf{0} & \mathbf{0} & \mathbf{0} \end{bmatrix},$$

$$\mathbf{K} = \begin{bmatrix} \mathbf{K}_{gg} & \mathbf{K}_{gc} & \mathbf{0} & \mathbf{K}_{gt} & \mathbf{0} \\ \mathbf{K}_{cg} & \mathbf{K}_{cc} & \mathbf{0} & \mathbf{K}_{ct} & \mathbf{0} \\ \mathbf{K}_{\omega g} & \mathbf{K}_{\omega c} & \mathbf{K}_{\omega\omega} & \mathbf{K}_{\omega t} & \mathbf{0} \\ \mathbf{K}_{tg} & \mathbf{K}_{tc} & \mathbf{0} & \mathbf{K}_{tt} & \mathbf{0} \\ \mathbf{K}_{ug} & \mathbf{K}_{uc} & \mathbf{0} & \mathbf{K}_{ut} & \mathbf{K}_{uu} \end{bmatrix},$$

$$\mathbf{x} = \left\{ \bar{\mathbf{p}}^g \; \bar{\mathbf{p}}^c \; \bar{\omega} \; \bar{\mathbf{T}} \; \bar{\mathbf{u}} \right\}^T.$$

The coefficients appearing in matrices K_{ij}, C_{ij}, f_i depend on primary variables so that Eqs. (20) are non-linear. They are given in detail in [4, 9].

The time discretization is done by means of the fully implicit Finite Difference Method (backward Euler algorithm),

$$\boldsymbol{\Psi}^i(\mathbf{x}_{n+1}) = \mathbf{C}_{ij}(\mathbf{x}_{n+1}) \frac{\mathbf{x}_{n+1} - \mathbf{x}_n}{\Delta t} + \mathbf{K}_{ij}(\mathbf{x}_{n+1})\, \mathbf{x}_{n+1} - \mathbf{f}_i(\mathbf{x}_{n+1}) = \mathbf{0}, \tag{21}$$

where $i, j = \mathrm{g}, \mathrm{c}, \omega, T, \mathbf{u}, n$ – time step number and Δt – time step length.

The set of differential, non-linear equations (21) is solved by means of a monolithic Newton–Raphson type iterative procedure [11],

$$\boldsymbol{\Psi}^i(\mathbf{x}^l_{n+1}) = -\left.\frac{\partial \boldsymbol{\Psi}^i}{\partial \mathbf{x}}\right|_{\mathbf{x}^l_{n+1}} \Delta \mathbf{x}^l_{n+1}, \qquad \mathbf{x}^{l+1}_{n+1} = \mathbf{x}^l_{n+1} + \Delta \mathbf{x}^l_{n+1}, \tag{22}$$

where l – iteration index.

5. Verification of the model

To verify the formulated mathematical model and to test the developed computer code two benchmark problems were simulated. The former is the well-known Henry's problem, which describes the advance of the saltwater front in a confined aquifer. Initially the aquifer is fully saturated with the pure water. Then the transport process is driven by the gradient of water density due to salt presence on one edge of the aquifer. The latter describes the capillary suction of salt in a water solution in the sandstone specimen. The experiment was performed in the Fraunhofer Institute for Building Physics and is described by Rucker *et al.* [12].

The first one is a two-dimensional problem, commonly used for benchmarking the density-driven models [13]. Henry's problem is unique because an analytical solution exists: however, Henry's analytical solution is rather controversial [13]. Therefore, in this paper the modified Henry's problem is used as the standard benchmark problem.

The idealized aquifer for simulation of Henry's problem is shown in Fig. 1. The porous domain is confined by its boundary, which on one side is subjected to a horizontal freshwater recharge. The freshwater exits toward a sea boundary composed of freshwater overlaying heavier seawater. All model parameters which are used to simulate the Henry's problem are: coefficient of molecular diffusion $D^{\mathrm{mol}} = 1.886 \cdot 10^{-5}\,[\mathrm{m^2 s^{-1}}]$, intrinsic permeability of porous material $k = 1.019 \cdot 10^{-9}\,[\mathrm{m^2}]$, recharge rate $q = 6.6 \cdot 10^{-5}\,[\mathrm{ms^{-1}}]$, porosity $n = 0.35$ and water properties as described in the previous section.

After carrying out numerical simulations, when the density field is stationary, the results in Fig. 2. are obtained. The figure shows the 0.25, 0.50, 0.75 isolines of relative salt concentrations. The results seem to be satisfactory when compared with the ones obtained by other authors [13].

The second benchmark test concerns suction experiment. The correctness of the presented model and software was proved by the comparison of the calculated results with experimental data [12]. Bottom surface of an initially almost dry sample, made of sandstone, was put into saturated salt (NaCl) in water solution. The parameters describing the materials are as follows: sandstone density $\rho^{\mathrm{s}} = 2120\,\mathrm{kg/m^3}$, porosity $n = 17\%$, intrinsic permeability $k = 1.5 \cdot 10^{-15}\,\mathrm{m^2}$, salt diffusion coefficient

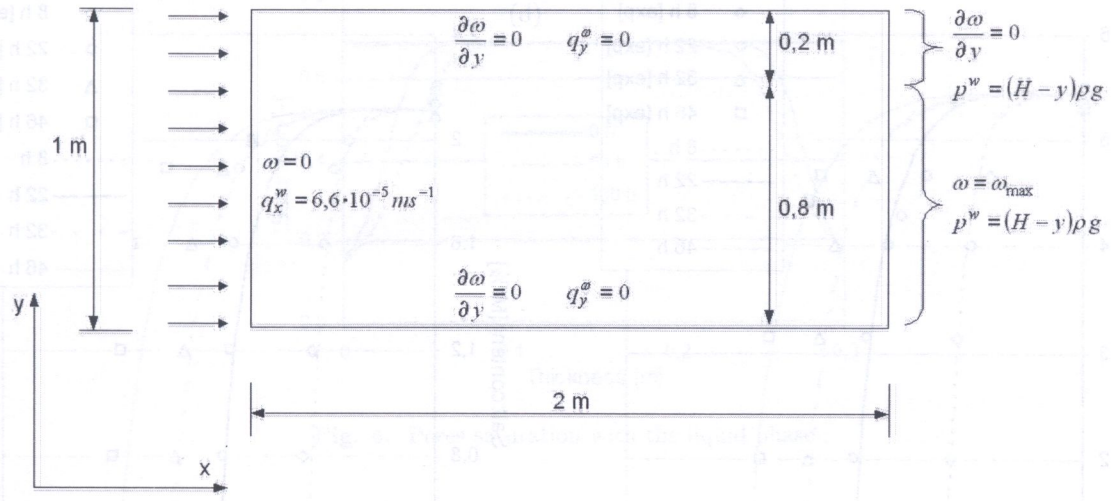

Fig. 1. Boundary conditions applied for solving Henry's salt-water intrusion problem

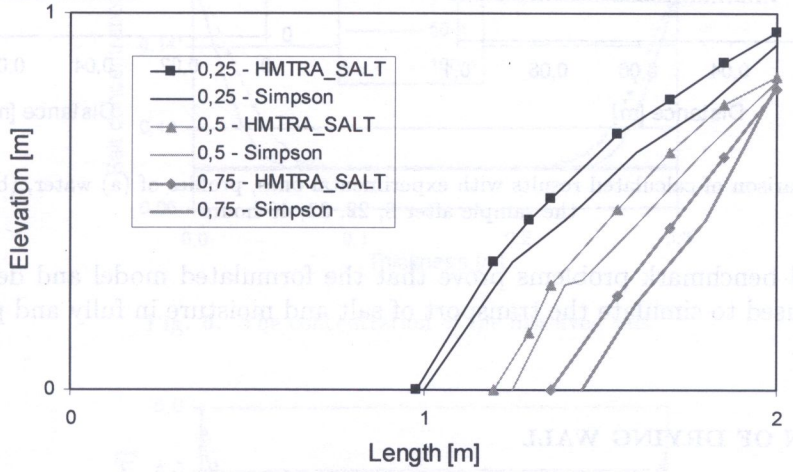

Fig. 2. Relative concentration field for Henry's problem

$D^{\text{mol}} = 10^{-9}$ m/s. The solution was sucked into pores due to capillary forces, which occur in partially saturated porous materials. The capillary suction in the sample was observed by upwards movement of saturation front. The salt and water content in the sample was measured using combinations of two non-destructive techniques: nuclear magnetic resonance (NMR) and gamma ray absorption. The NMR takes advantage of the fact that the amount of energy absorbed by the specimen depends on the number of protons in the specimen. Because the hydrogen nuclei in building materials occur only in the form of water, NMR can be used to measure moisture content. Gamma ray absorption employs the fact that photons from radioactive source (241Am, 137Cs, 60Co) interact with matter. The attenuation of gamma ray registers the absorption of photons, penetrating the sample, by water and salt particles. By combination of these two techniques both the moisture and salt profile may be determined. The test was performed in Fraunhofer Institute for Building Physics. Both NMR and gamma ray absorption were used to measure moisture and salt content. This experiment was also modelled and solved using the developed computer code. The comparison of the results calculated using HMTRA_SAL with the results obtained in laboratory test is presented in Fig. 3.

Figure 3a shows water, and Fig. 3b salt content profile after 8, 22, 32, 46 hours. As it is visible in the above graphs, the calculated results are in good agreement with the experimental data.

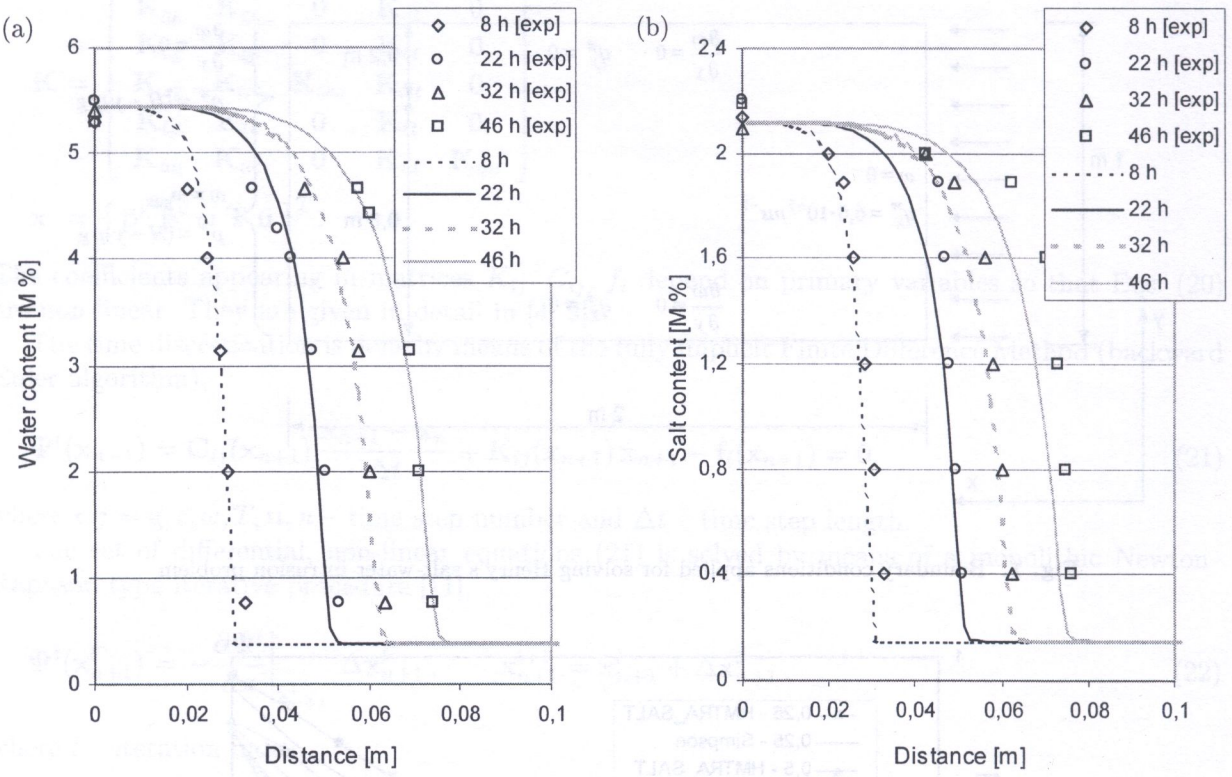

Fig. 3. Comparison of calculated results with experimental ones, profiles of (a) water, (b) salt content in the sample after 8, 22, 32, 46 hours

The presented benchmark problems prove that the formulated model and developed computer program can be used to simulate the transport of salt and moisture in fully and partially saturated porous materials.

6. Simulation of drying wall

A process of wall drying, which occurs usually in spring, when water evaporates from a building element after winter, has been simulated. It will be shown that during the drying of the wall, salt may precipitate nearby the surface. Therefore, efflorescence on the surface and additional pressure exerted on the material skeleton can be observed. These phenomena are responsible for damage of valuable historical surfaces as frescos and paintings.

The wall has been modelled as a 1D domain, 30 cm thick. The material is characterised by the following properties: porosity $n = 0.12$, intrinsic permeability $k = 3.0 \cdot 10^{-21}\,\mathrm{m}^2$. Water sorption isotherms are described by the following equation,

$$p^{\mathrm{c}}(S_{\mathrm{w}}) = a(S_{\mathrm{w}}^{-b} - 1)^{1-1/b}. \tag{23}$$

The balance between dissolved and precipitated salt is modelled by the Freundlich type sorption isotherm given by

$$S_{\mathrm{p}} = \alpha S_{\mathrm{w}} \omega^{\beta} \tag{24}$$

where α and β are material parameters.

Initially, the wall is partially saturated with water, $S_{\mathrm{w}} = 0.69$ (relative humidity = 80%), the concentration of dissolved salt is homogeneous along the thickness of the wall, $\omega = 0.08\,[\mathrm{kg/kg}]$. Temperature is constant during the experiment time, $T = 20°\mathrm{C}$. The relative humidity of surrounding air suddenly decreases from its initial value till 20%. The water starts to evaporate, but salt

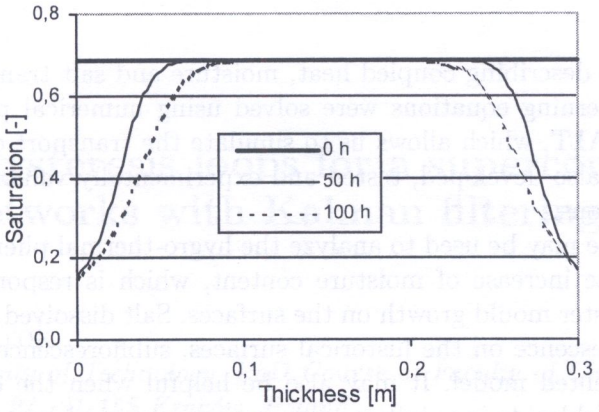

Fig. 4. Pores saturation with the liquid phase

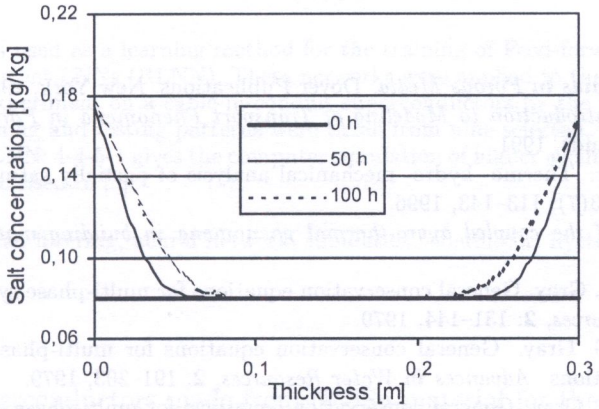

Fig. 5. The concentration of the dissolved salt

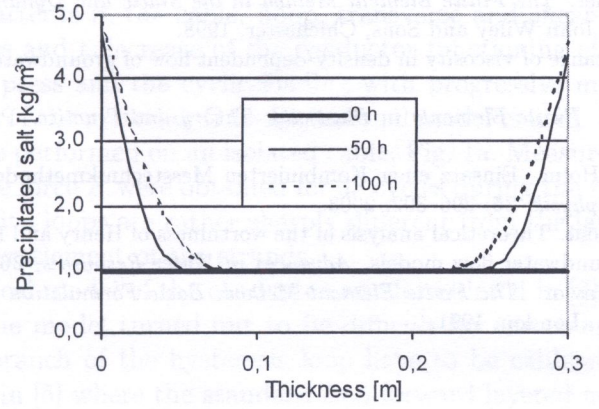

Fig. 6. The density of precipitated salt

remains in the pores. The boundary condition for the mass exchange is of the third type (Cauchy's BC). Water is transported towards the wall surfaces, where it is evaporating. The profile of pores saturation with the liquid phase is changing during the drying process – Fig. 4. Salt was transported toward the surfaces of the wall with water. Near the surfaces both the dissolved salt concentration and the mass of precipitated salt are rapidly increasing.

The profiles of the dissolved salt concentration and the density of precipitated salt are changing during the drying process – Figs. 5 and 6.

7. Conclusions

The mathematical model describing coupled heat, moisture and salt transport in porous materials was formulated. The governing equations were solved using numerical procedures (FEM, FDM). The software HMTRA-SALT, which allows us to simulate the transport of heat, moisture and salt in porous materials, was also developed, tested and experimentally validated, both for full and for partial saturation conditions.

The developed software may be used to analyze the hygro-thermal phenomena in salted building envelopes. Salt causes the increase of moisture content, which is responsible for the decrease of thermal resistance and faster mould growth on the surfaces. Salt dissolved in water and precipitated in the pores causes efflorescence on the historical surfaces, subflorescence (spalling), which can be predicted using the presented model. It may also be helpful when the damage of the structures caused by containments (chloride ions initiate the corrosion of steel bars, leaching which degrades the strength properties of a material) is assessed.

References

[1] J. Bear. *Dynamics of Fluids in Porous Media.* Dover Publications, New York, 1988.

[2] J. Bear, Y. Bachmat. *Introduction to Modeling of Transport Phenomena in Porous Media.* Kluwer Academic Publishers, The Netherlands, 1991.

[3] D. Gawin, B.A. Schrefler. Thermo- hydro- mechanical analysis of partially saturated porous materials. *Engineering Computations*, **13**(7): 113–143, 1996.

[4] D. Gawin. *Modelling of the coupled hygro-thermal phenomena in building materials* (in Polish). Technical University of Łódź, 2000.

[5] S.M. Hassanizadeh, W.G. Gray. General conservation equations for multi-phase system: 1. Averaging procedure. *Advances in Water Resources*, **2**: 131–144, 1979.

[6] S.M. Hassanizadeh, W.G. Gray. General conservation equations for multi-phase system: 2. Mass, momenta, energy and entropy equations. *Advances in Water Resources*, **2**: 191–203, 1979.

[7] S.M. Hassanizadeh, W.G. Gray. General conservation equations for multi-phase system: 3. Constitutive theory for porous media flow. *Advances in Water Resources*, **3**: 25–40, 1980.

[8] S.M. Hassanizadeh, T. Leijnse. On the modeling of brine transport in porous media. *Water Resource Research*, **3**: 321–330, 1988.

[9] R.W. Lewis, B.A. Schrefler. *The Finite Element Method in the Static and Dynamic Deformation and Consolidation of Porous Media.* John Wiley and Sons, Chichester, 1998.

[10] D.U. Ophori. The significance of viscosity in density-dependent flow of groundwater. *Journal of Hydrology*, **204**: 261–270, 1998.

[11] D.R.J. Owen, E. Hinton. *Finite Elements in Plasticity: Theory and Practice.* Pineridge Press Ltd., Swansea, 1980.

[12] P. Rucker, M. Krus, A. Holm. Einsatz einer Kombinierten Messtechnikmethode zur Untersuchung von Salztransportvergangen. *Bauphysik*, **25**: 296–302. 2003.

[13] M.J. Simpson, T.P. Clement. Theoretical analysis of the worthiness of Henry and Elder problems as benchmarks of density-dependent groundwater flow models. *Advances in Water Resources*, **26**: 17–31. 2003.

[14] O.C. Zienkiewicz, R.L. Taylor. *The Finite Element Method. Basic Formulation and Linear Problems*, 4th ed, Vol. 1. McGraw-Hill Ltd., London, 1991.